J|A|C|S
ARTICLES
Published on Web 06/06/2002

Functionalizable Polycyclic Aromatics through Oxidative Cyclization of Pendant Thiophenes

John D. Tovar, Aimee Rose, and Timothy M. Swager*

Contribution from the Department of Chemistry and the Center for Materials Science and Engineering, Massachusetts Institute of Technology, Cambridge, Massachusetts 02139

Received March 21, 2002

Abstract: We present a general strategy for obtaining large sulfur-containing polycyclic aromatics from thienyl precursors through iron(III) chloride mediated oxidative cyclizations. By placing thienyl moieties in close proximity to adjacent arenes, we have directed the oxidized intermediates into controlled cyclization pathways, effectively suppressing polymer formation. Utilizing these cyclized compounds and their thienyl precursors, we have studied cyclization/polymerization pathways of polymers such as poly(**2**). The unsubstituted positions α to the sulfur atoms within these aromatic cores allowed for efficient halogenation and further functionalization. As a demonstration, we prepared a series of arylene−ethynylene polymers with varying degrees of chromophore aromatization and used them to probe the effects of synthetically imposed rigidity on polymer photophysical behavior. The symmetries and effective conjugation pathways within the monomers play a key role in determining photophysical properties. We observed that rigid, aromatized chromophores generally led to increased excited-state lifetimes by decreasing radiative rates of fluorescence decay.

Introduction

Thiophene-based electronic materials have engendered significant interest from the standpoint of new synthetic methodologies and improved material properties.[1] Research initially focused on polythiophenes since a "bridging sulfur" could effectively provide aromatic stability to polyacetylene while preserving desirable physical properties such as high conductivity.[2] The facile functionalization of a thiophene monomer offers relatively efficient synthetic solutions to band-gap tuning, solubility, and processability.[1b] Earlier research on charge-transfer conductors revealed the role of sulfur as an atom having greater radial extension in its bonding thus enhancing cofacial electronic interactions between stacked molecules. The incorporation of sulfur into polycyclic aromatic frameworks has also met considerable success as applied to the design and synthesis of unique organic semiconductors that exhibit gate-induced field effects. For example, synthetic efforts led by Katz and by Müllen have utilized variants of polycyclic aromatic hydrocarbon chemistry to obtain fully aromatized, sulfur-containing aromatics exhibiting p-type field-effect mobilities of up to 0.15 cm^2/Vs.[3,4]

The study of oxidative carbon−carbon bond formation as a means of constructing discrete thiophene-based polycyclics has received little attention when compared to the reliance on this method for the synthesis of polythiophenes.[1c] Arene cyclizations induced by chemical oxidants have successfully led to the construction of aromatized ring structures as diverse as four-ring triphenylenes and 91-ring planar graphitic sheets.[5,6] On the other hand, prior to our studies, the highly reactive nature of oxidized thiophene moieties has not allowed for the development of well-defined, thiophene-centered oxidative cyclizations. Such oxidized monomers often polymerize rather than undergo discrete monomer cyclizations.[1c,7] Photochemical Mallory-type cyclizations in the presence of oxidants such as iodine, an important variant of this strategy, often provide poor yields of aromatized thiophenes when compared to their benzo bretheren due to aryl migrations and formation of reactive thiyl radicals.[8]

Recently, we described a tandem cyclization/polymerization strategy from pendant monomer **1** where we could selectively form an aromatized naphtho[2,1-*b*:3,4-*b*′]dithiophene such as **2** through chemical or electrochemical oxidation of an appropriately substituted thienyl monomer prior to further polymer growth (Scheme 1).[9] We report herein that this general procedure allows for the synthesis of a variety of electroactive thiophene-based materials. We present the synthesis of model compounds

* To whom correspondence should be addressed. E-mail: tswager@mit.edu.

(1) (a) *Handbook of Conducting Polymers*, 2nd ed.; Skotheim, T. A., Elsenbaumer, R. L., Reynolds, J. R., Eds.; Marcel Dekker: New York, 1998. (b) Roncali, J. *Chem. Rev.* **1997**, *97*, 173−205. (c) McCullough, R. D. *Adv. Mater.* **1998**, *10*, 93−116.
(2) Tourillon, G.; Garnier, F. *J. Electroanal. Chem.* **1982**, *135*, 173−178.
(3) Laquindanum, J. G.; Katz, H. E.; Lovinger, A. J. *J. Am. Chem. Soc.* **1998**, *120*, 664−672.
(4) Sirringhaus, H.; Friend, R. H.; Wang, C.; Leuninger, J.; Müllen, K. *J. Mater. Chem.* **1999**, *9*, 2095−2101.
(5) Matheson, I. M.; Musgrave, O. C.; Webster, C. J. *Chem. Commun.* **1965**, 278−279.
(6) Iyer, V. S.; Wehmeier, M.; Brand, J. D.; Keegstra, M. A.; Müllen, K. *Angew. Chem., Int. Ed. Engl.* **1997**, *36*, 1604−1607.
(7) See for example: Naudin, E.; El Mehdi, N.; Soucy, C.; Breau, L.; Bélanger, D. *Chem. Mater.* **2001**, *13*, 634−642.
(8) (a) Mallory, F. B.; Mallory, C. W. *Org. React.* **1984**, *30*, 1−456. For specific examples of 3-thienyl decomposition and photoisomerizations, see: (b) Wynberg, H.; van Driel, H.; Kellogg, R. M.; Buter, J. *J. Am. Chem. Soc.* **1967**, *89*, 3487−3494. (c) Kellogg, R. M.; Groen, M. B.; Wynberg, H. *J. Org. Chem.* **1967**, *32*, 3093−3100.
(9) Tovar, J. D.; Swager, T. M. *Adv. Mater.* **2001**, *13*, 1775−1780.

10.1021/ja0262636 CCC: $22.00 **© 2002 American Chemical Society**

Scheme 1

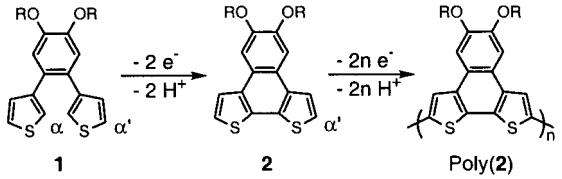

Scheme 2

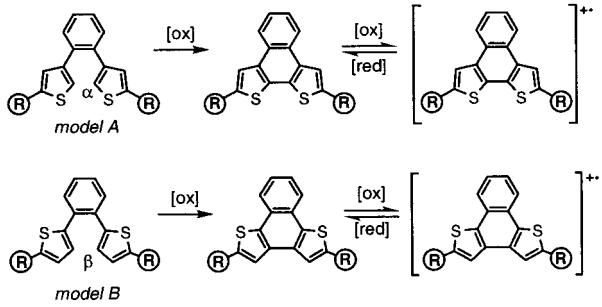

that provide convincing electrochemical evidence in support of our cyclization/polymerization scheme. These polycyclic aromatics allow for further functionalization at positions α to the sulfur atoms and ultimately for incorporation into new extended molecular and polymeric systems. Through such elaboration, we will present the effects of chromophore aromatization on polymer photophysical behavior and utilize molecular models to further corroborate this effect.

Results and Discussion

Synthetic and Electrochemical Studies. Our initial work sought to verify the connectivity of polymeric materials such as poly(**2**) and to shed light on the tandem cyclization/polymerization sequence shown in Scheme 1. To accomplish this, we needed models that would participate in electrochemically mediated cyclization events without undergoing oxidative polymerization. We envisioned that the generic structural motifs presented in Scheme 2 would serve in this capacity. Model A has pendant 3-thienyl rings with blocking groups at the 5-position α-sites to prevent polymerization. For the substitutional isomer, we chose model B, where the pendant 2-thienyl rings also have blocking groups on the polymerizable α-sites. If polymer growth indeed propagates through the sites now blocked in these models, cyclic voltammetry (CV) should detect the redox activities of any new electroactive species formed at the electrode rather than irreversible follow-up chemical polymerization. Furthermore, these models would shed light on the propensities (if any) toward coupling defects through vacant aryl or *β*-thienyl sites on the aromatized models. Systematically addressing these reactive sites allows us to probe the observed reactivity while maintaining a close degree of structural similarity to **1** and the resulting poly(**2**). In our previous studies, we found that monomer **1** exhibited two anodic peaks during successive cyclic sweeping, while chemically α−α cyclized monomer **2** displayed only one signal that corresponded well to the second peak observed for **1**.[9] Here, we electrochemically examine the first step of the polymerization with substrates that should not polymerize.

Using standard thiophene halogenation chemistry and Suzuki cross-coupling techniques,[10] we obtained the α′-blocked, non-

(10) Miyaura, N.; Yanagi, T.; Suzuki, A. *Synth. Commun.* **1981**, *11*, 513−519.

Scheme 3[a]

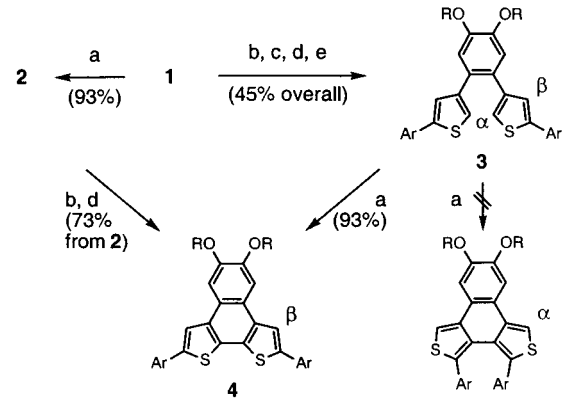

[a] R = *n*-$C_{14}H_{29}$, Ar = 2,5-$Me_2C_6H_3$-. Reagents and conditions: (a) $FeCl_3$, CH_2Cl_2; (b) Br_2, CH_2Cl_2; (c) $PhI(OCOCF_3)_2$, I_2, CCl_4 (no light); (d) $ArB(OH)_2$, $Pd(PPh_3)_4$, Na_2CO_3, PhMe/EtOH/H_2O; (e) i. *n*-BuLi, THF, −78 °C; ii. AcOH, −78 °C to room temperature.

polymerizable **3** as an example of model A. As outlined in Scheme 3, bromination occurred regioselectively at the α-positions of **1**, and subsequent iodination occurred at the remaining α′-positions.[11] Although the high reactivity of both thienyl halides provided low chemoselectivity for the Suzuki cross-coupling, we obtained modest yields of the desired iodo-coupled product corresponding to aryl installation at the α′-site. Finally, debromination via lithium−halogen exchange provided the α-unsubstituted **3**. To assess the specificity of the oxidative cyclization under chemical conditions, we subjected **3** to $FeCl_3$ oxidation and obtained **4** in high yield. We could employ several molar excesses of oxidant to drive the reaction to completion without apparent dimerization or polymerization. Remarkably, this reaction provided only one product, indicating that the α−α sites of **3** had participated in the cyclization.[12] To verify this assignment, we performed a parallel synthesis from **2**. Bromination of the α′-sites of **2** followed by Suzuki coupling yielded an identical product to that obtained through oxidative cyclization of **3**. This verifies that in the presence of both vacant α- and *β*-positions of **3**, the more reactive α-sites indeed participate in the cyclization to afford **4** selectively and in high yield. We observed no evidence for the formation of the hypothetical *β*−*β* coupling product shown in Scheme 3.

Analysis of **3** and **4** by CV revealed corroborating oxidation activity. Both **3** and **4** shared reversible redox characteristics when swept at 100 mV/s (Figure 1): **3** exhibited two redox waves with half-wave potentials ($E_{1/2}$) of 0.86 and 1.31 V while **4** displayed two redox waves with $E_{1/2}$ values of 0.88 and 1.28 V. The lower potential anodic wave observed for **3**, with an anodic peak potential (E_{pa}) of 0.93 V, appeared much stronger and broader than that for **4**, indicating a possible superposition of an irreversible oxidation and a reversible redox couple. Indeed, slower scans (25 mV/s) through the first half-wave potential of both compounds helped to better resolve this difference (insets of Figure 1). These data clearly show two distinct oxidations occurring within the first broad redox wave of **3** (top inset): one irreversible oxidation with an E_{pa} of 0.85

(11) D'Auria, M.; Mauriello, G. *Tetrahedron Lett.* **1995**, *36*, 4883−4884.
(12) Five aromatic resonances appeared in the ^{1}H NMR of **4**, three of which we assigned to the pendant 2,5-dimethylphenyl moieties. The two remaining singlets, reflecting a high degree of molecular symmetry, indicated either an α−α or a *β*−*β* coupling.

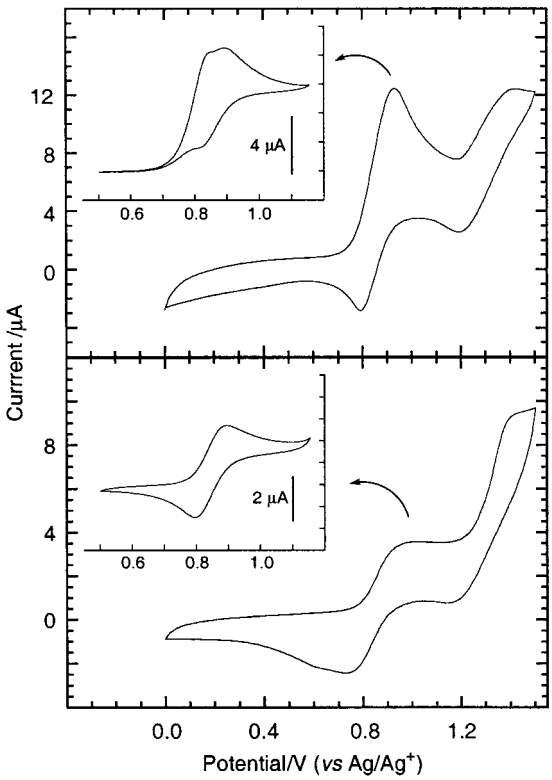

Figure 1. Cyclic voltammetry of **3** (top, 1.2 mM) and **4** (bottom, 1.0 mM) at a 2 mm^2 Pt button electrode in 0.1 M *n*-Bu_4PF_6 (CH_2Cl_2) scanned at 100 mV/s; inset scans were taken at 25 mV/s. $E_{1/2}(Fc/Fc^+) = +222$ mV.

V and one reversible couple with an $E_{1/2}$ of 0.85 V ($E_{pa} = 0.89$ V, peak−peak separation $\Delta E_p = 88$ mV). In comparison, **4** only exhibits the redox wave with an $E_{1/2}$ of 0.85 V (bottom inset; $E_{pa} = 0.90$ V, $\Delta E_p = 98$ mV).[13]

In line with the independent chemical syntheses of **4**, the initial oxidation of **3** leads to an intramolecular α−α cyclization. Subsequent deprotonation and rearomatization leads to **4**, and this product undergoes reversible redox chemistry at a higher potential essentially identical with that displayed by the chemically synthesized **4**. With the α′-sites blocked, we observed no evidence for irreversible chemical follow-up reactions upon oxidation (e.g. dimerization). In the absence of aryl groups blocking the reactive α′-positions of **4**, radical cations derived from such an electrode-aromatized product (e.g. $\mathbf{2}^{\bullet+}$) then engage in follow-up chemical couplings and subsequent growth of poly-(**2**) as opposed to the reversible redox chemistry observed for the blocked model.

As the cyclization/polymerization reactivity depicted in Scheme 1 also applied to the substitutional α-linked thiophene isomers, we sought to explore the electrochemical activity of nonpolymerizable α-thienyl derivatives such as **5** (model B), readily obtained through Stille cross-coupling (Scheme 4).[14] Unlike **3**, methyl-blocked **5** only has one vacant site available for oxidative cyclization that would lead to an aromatized system. Accordingly, chemical oxidation of **5** furnished the naphthodithiophene **6** in modest yield. Both **5** and **6** provided

Scheme 4[a]

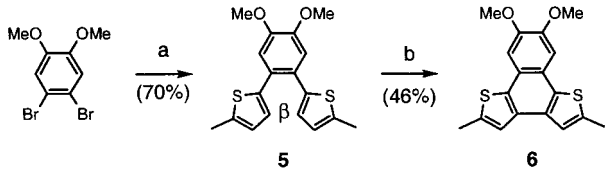

[a] Reagents and conditions: (a) 5-methyl-2-tributylstannyl thiophene, $(Ph_3P)_2PdCl_2$, DMF, 80 °C; (b) $FeCl_3$, CH_2Cl_2, room temperature.

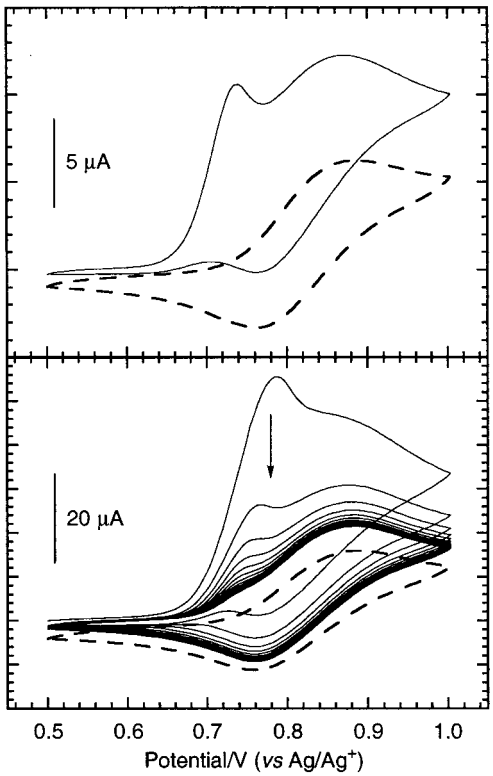

Figure 2. Cyclic voltammetry of **5** (—, 1.1 mM) and **6** (- -, 1.2 mM) at a 2 mm^2 Pt button electrode in 0.1 M *n*-Bu_4PF_6 (CH_3CN) scanned at 100 mV/s (top) and at 750 mV/s (bottom); $E_{1/2}(Fc/Fc^+) = +84$ mV.

distinct electrochemical signatures that also shed light into the general mechanism of Scheme 1 (Figure 2, top).

The CV of **5** displayed two strong oxidation peaks at 100 mV/s scan rates (solid line): one irreversible wave with an E_{pa} of 0.74 V attributed to oxidation of the pendant thienyl ring of **5** followed by a $\beta-\beta$ chemical cyclization and deprotonation process, and one well-defined and reversible redox wave with an $E_{1/2}$ of 0.82 V ($E_{pa} = 0.87$ V, $\Delta E_p = 110$ mV) attributed to electrochemical formation of a stable radical cation species. Subjecting **6** to the same conditions provided the reversible redox process only with an $E_{1/2}$ of 0.82 V (dashed line: $E_{pa} = 0.89$ V, $\Delta E_p = 130$ mV). Furthermore, repetitive fast CV scans of **5** at 750 mV/s resulted in a decrease in intensity for the initial oxidative peak ($E_{pa} = 0.79$ V) followed by a *pseudo*-steady-state buildup of an electrochemically active product in the vicinity of the electrode (Figure 2, bottom). This *quasi*-reversible redox couple, with an $E_{1/2}$ at 0.82 V ($E_{pa} = 0.89$ V, $\Delta E_p = 130$ mV), resembled that obtained independently through fast scan sweeps of **6** (Figure 2, bottom; dashed line). As with **3** and **4**, we observed no evidence for dimerization or polymer growth with continued cyclic sweeping through oxidizing potentials. In total, the data for **3**−**4** and for **5**−**6** support a coupled and electrochemically mediated cyclization/polymerization process,

(13) Although a formally reversible one-electron redox couple requires a peak-to-peak separation of 59 mV, we observed similar broadening behavior under identical conditions for the known, reversible one-electron ferrocene/ferrocenium couple. For another recent observation of such nonnernstian behavior in aprotic solvents, see: Lai, R. Y.; Fabrizio, E. F.; Lu, L.; Jenekhe, S. A.; Bard, A. J. *J. Am. Chem. Soc.* **2001**, *123*, 9112−9118.

(14) Milstein, D.; Stille, J. K. *J. Am. Chem. Soc.* **1979**, *101*, 4992−4998.

Scheme 5[a]

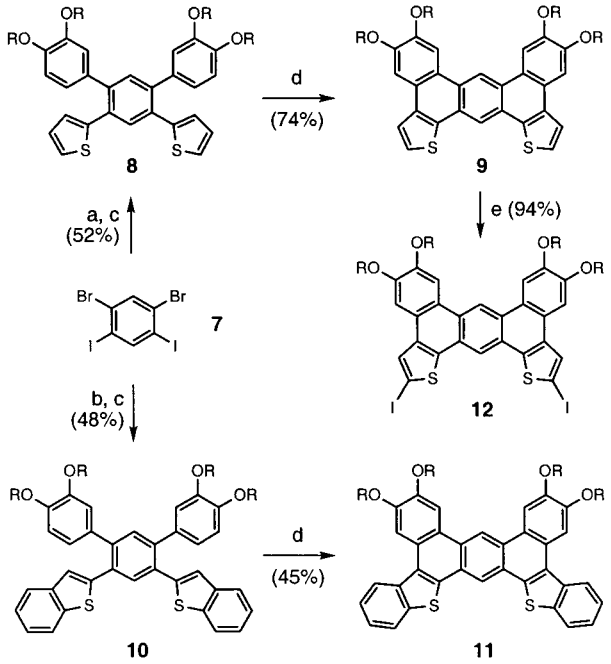

[a] R = 2-ethylhexyl. Reagents and conditions: (a) 2-tributylstannyl thiophene, $(Ph_3P)_2PdCl_2$, DMF, 80 °C; (b) 2-tributylstannyl benzo[*b*]-thiophene, $(Ph_3P)_2PdCl_2$, DMF, 80 °C; (c) 3,4-di(2-ethylhexyloxy)phenylpinacolatoborane, $Pd(PPh_3)_4$, Na_2CO_3, PhMe, EtOH, H_2O, 90 °C; (d) $FeCl_3$, CH_2Cl_2, room temperature; (e) i. *n*-BuLi, TMEDA, THF −78 °C; ii. I_2, −78 °C to room temperature.

where the oxidized form of a monomer initially cyclized in situ (such as **2**) participates in intermolecular couplings leading to polymer growth through the remaining unsubstituted sites α to the sulfur atoms.

Using the examples of efficient thienyl-based carbon−carbon bond formation from above, we utilized oxidative cyclizations to construct larger systems via thienyl-*aryl* carbon−carbon bond formation. From the versatile halide scaffold **7**,[15] chemoselective cross-coupling under palladium catalysis provided the differentially substituted pendant monomer **8** via sequential Stille and Suzuki cross-couplings (Scheme 5, top). In an experimentally similar oxidation protocol used for constructing **2**, **4**, and **6** ($FeCl_3/CH_2Cl_2$), pendant compound **8** readily cyclized to construct the extended aromatic system **9** in respectable yield; however, the significant excesses of iron oxidant required to drive the cyclization to completion also led to some decomposition.

Analogous to **5** and **6**, repetitive fast scan CVs at 750 mV/s with **8** indicated one E_{pa} at 1.32 V, and successive scans eventually reached a *pseudo*-steady-state voltammogram exhibiting two reversible waves with $E_{1/2}$ values of 0.84 (E_{pa} = 0.95 V, ΔE_p = 220 mV) and 1.11 V (E_{pa} = 1.23 V, $\Delta E_p \approx$ 200 mV; Figure 3). For comparison, the CV of **9** under identical conditions exhibited two reversible processes with $E_{1/2}$ values of 0.83 (E_{pa} = 0.96 V, ΔE_p = 240 mV) and 1.11 V (E_{pa} = 1.23 V, ΔE_p = 230 mV; Figure 3, dashed line). This indicates the buildup of a new electroactive species at the working electrode resulting from an oxidatively induced aryl−thienyl bond formation. When compared to **3**, the more positive initial E_{pa} for **8** reflects the lesser degree of electronic induction afforded by the pendant alkoxy groups. This results from the additional

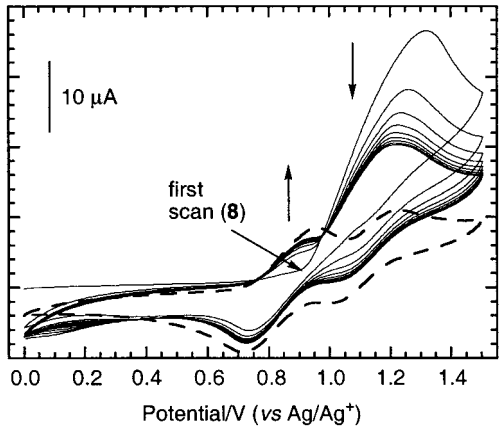

Figure 3. CVs of **8** (—, 1.0 mM) and **9** (- -, 1.1 mM) scanned at 750 mV/s with conditions as in Figure 1; $E_{1/2}(Fc/Fc^+)$ = +230 mV.

phenylene spacer placed between the dialkoxy arene and the thienyl moiety. After cyclization, **9** then exhibits two reversible oxidations at less positive potentials than in **8** due to the stabilization offered by a completely aromatized system.

To demonstrate generality, we examined if extended benzannulation on the thiophene moiety would affect the cyclization efficiency. We prepared model compound **10** through similar cross-coupling strategies used for **8**, where benzo[*b*]thiophen-2-yl groups in **10** replace the thienyl groups of **8** (Scheme 5, bottom). Similar oxidative conditions provided the doubly cyclized **11** in moderate yield. As with the conversion to **9**, extensive decomposition occurred during $FeCl_3$-promoted cyclization, and the reaction mixture proved difficult to purify. Although efforts to further functionalize **11** have not yet met with success, the utilization of this chemistry onto larger heteroaromatics indicated that such oxidative cyclizations extend beyond simple thiophene derivatives. Owing to the favorable cofacial interactions possible between such large planar π-systems, fused compounds **9** and **11** exhibited concentration-dependent ^{1}H NMR shifts as expected for a strongly aggregating system. We anticipate that this propensity will allow for extended intermolecular organization, making more crystalline derivatives of **9** and **11** suitable for organic field-effect transistor (OFET) applications.

Repetitive fast scan CV cycling appeared to indicate an efficient conversion of **10** to **11** although undesired electrode passivation at higher potentials complicated CV analysis. The CVs of very dilute samples of **10** (ca. 0.09 mM) provided only capacitive current until sweeping through the initial E_{pa} at 1.11 V. Subsequent scans revealed a less-positive potential redox couple with an $E_{1/2}$ of 0.78 V (E_{pa} = 0.84 V, ΔE_p = 120 mV) and a concurrent decrease in anodic current of the higher potential oxidation step, analogous to **8** (Figure 4, top). In comparison, we observed a similar redox couple for very dilute solutions of **11** with an $E_{1/2}$ at 0.75 V (E_{pa} = 0.83 V, ΔE_p = 150 mV; Figure 4, bottom); again, sweeping in solutions on the order of 1 mM at more positive potentials also led to passivation. Future efforts will incorporate more stable units with stronger aromaticity to foster greater electrochemical reversibility.

Incorporation into Conjugated Polymers. We found that unsubstituted positions α to the sulfur provided synthetic handles to allow for incorporation into even larger systems in analogy to the readily halogenated core of **2**.[9] For example, the α-sites

(15) Hart, H.; Harada, K.; Du, C.-J. F. *J. Org. Chem.* **1985**, *50*, 3104−3110.

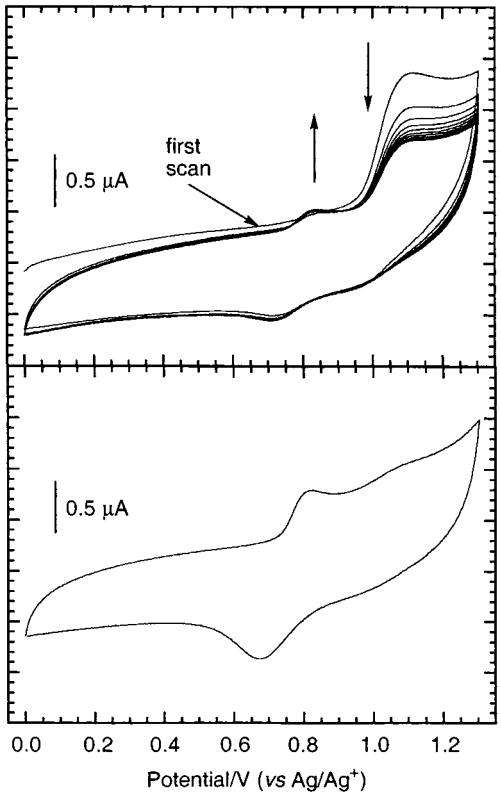

Figure 4. CVs of **10** (repetitive scans, top, ca. 0.09 mM) and **11** (bottom, ca. 0.22 mM) taken at 500 mV/s, with conditions as in Figure 1; $E_{1/2}$(Fc/Fc$^+$) = +231 mV.

of **9** iodinated in very high yield after double lithiation and iodine trapping to provide **12** (Scheme 5). Halogenation proceeded regioselectively to the α-sites as determined by ROESY spectroscopy. From a molecular standpoint, facile functionalization of a large aromatic core has important implications for the development of new molecular architectures. Additional thiophene couplings will tune the redox potential while substitution with an unsaturated residue such as an alkynyl moiety will further delocalize the chromophore. For example, **12** readily participated in Sonogashira-type polymerizations with the diethynyl pentiptycene **13** to provide the fluorescent conjugated polymer **14** (Scheme 6, M_n = 16 500).[16,17]

Our recent studies on polymers comprised of triphenylene and dibenzo[*g*,*p*]chrysene units showed that larger aromatic cores facilitated exciton migration and provided longer excited-state lifetimes,[18] two key improvements necessary for optimizing sensory responses.[19] This earlier work specifically targeted the triphenylene chromophore due to its weakly forbidden low-energy transitions, a property often shared with other larger polycyclic aromatics. We anticipated that the extended planarity and rigidity of meta-oriented comonomer **12** would also offer a long-lived excited state; indeed, polymer **14** exhibited a lifetime of 1.06 ns in solution (CH_2Cl_2). When coupled with our earlier findings, this provides an additional and empirical demonstration of excited-state lifetime extension in that the

Scheme 6[a]

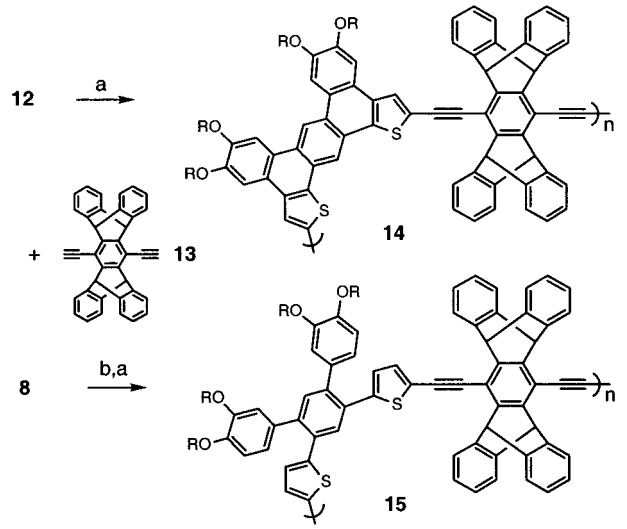

[a] R = 2-ethylhexyl. Reagents and conditions: (a) **13**, $Pd(PPh_3)_4$, CuI, PhMe, *i*-Pr_2NH, 85 °C; (b) i. $Hg(OAc)_2$, CH_2Cl_2; ii. I_2, room temperature.

dominant conjugation pathway through a dibenzochrysene or a triphenylene core has different geometric and electronic properties than that for **14**.

A systematic study of such large aromatic chromophores, one goal of the present work, would assess the relative photophysical contributions of molecular symmetry and planarity within conjugated polymer systems and would help to outline parameters required for more efficient sensory materials. Prior to our investigations, no molecular design precedents have established definite relations between chromophore rigidity and photophysical properties.[20] We sought to study these trends within polymeric systems of varied symmetries and structural constraints. The facile halogenations of both the pendant **8** and cyclized **9** prompted us to examine the effects of chromophore aromatization on the polymer's photophysical behavior. To this end, we synthesized the flexible, noncyclized polymer **15** after iodinating the meta precursor **8** directly (Scheme 6, bottom; M_n = 21 000). This polymer serves to maintain similar structural connectivity to **14** thereby allowing for comparison of the effects of chromophore aromatization. As a further application of thiophene-based controlled oxidative cyclizations, we examined the related para family of polymers (**16** and **17** in Scheme 7) with backbone electronic properties that again differ in the degree of comonomer aromatization imparted by two oxidatively formed carbon−carbon bonds.

The monomer synthetic scheme allowing entry into the para systems paralleled that used for constructing the meta system **8** (Scheme 7). Sequential Stille and Suzuki cross-couplings onto the isomeric para scaffold **18**[15] afforded the thienyl-substituted terphenyl **19** (X = H), and halogenation proceeded in high yield to provide dibromide **20** or diiodide **21**. At this point, **21** copolymerized with **13** under Sonogashira conditions to afford the pendant polymer **16** (M_n = 15 000). The oxidative conversion of **19** directly into the aromatized system failed due to unavoidable polymer formation,[21] in stark contrast to the

(16) Sonogashira, K.; Tohda, Y.; Hagihara, N. *Tetrahedron Lett.* **1975**, 4467−4470.
(17) Yang, J.-S.; Swager, T. M. *J. Am. Chem. Soc.* **1998**, *120*, 11864−11873.
(18) (a) Rose, A.; Lugmair, C. G.; Swager, T. M. *J. Am. Chem. Soc.* **2001**, *123*, 11298-11299. (b) Yamaguchi, S.; Swager, T. M. *J. Am. Chem. Soc.* **2001**, *123*, 12087−12088.
(19) Swager, T. M. *Acc. Chem. Res.* **1998**, *31*, 201−207.
(20) For examples concerning biphenyl and terphenyl derivatives of varying degrees of geometric restrictions, see: Nijegorodov, N. I.; Downey, W. S. *J. Phys. Chem.* **1994**, *98*, 5639−5643. While the rate of fluorescence decay in "planar" methylene-bridged biphenyl (fluorene) increased relative to biphenyl, the methylene-bridged terphenyl systems displayed the opposite effect with enhanced planarity.

Scheme 7[a]

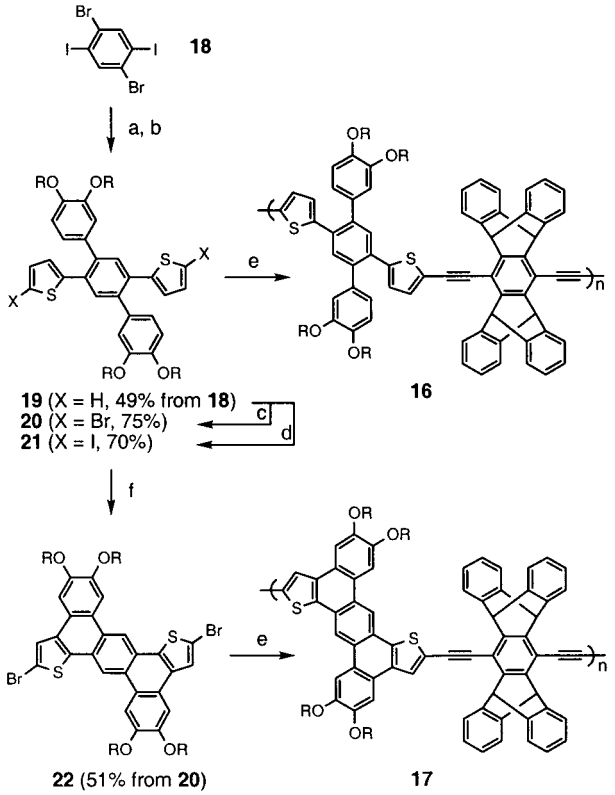

[a] R = 2-ethylhexyl. Reagents and conditions: (a) 2-tributylstannyl thiophene, $(Ph_3P)_2PdCl_2$, DMF, 80 °C; (b) 3,4-di(2-ethylhexyloxy)phenylpinacolatoborane, $Pd(PPh_3)_4$, Na_2CO_3, PhMe, EtOH, H_2O, 90 °C; (c) NBS, DMF, CH_2Cl_2, room temperature; (d) i. $Hg(OAc)_2$; ii. I_2, CH_2Cl_2, room temperature; (e) **13**, $Pd(PPh_3)_4$, CuI, PhMe, *i*-Pr_2NH, 85 °C; (f) $FeCl_3$, CH_2Cl_2, room temperature.

relatively clean cyclization of meta system **8** into **9**. Therefore, we hoped to prevent this by employing the halogens to block the reactive and polymerizable α-sites. The carbon−iodine bond lability of **21** apparently led to significant dehalogenation and dimerization during chemical cyclization as observed by mass spectrometry; however, bromide **20** cleanly cyclized under the $FeCl_3$ oxidation conditions to afford **22**. Despite the sparingly soluble nature of **22**, exhaustive purification of the crude product (and concomitant material losses) provided modest isolated yields. From **22**, we used Sonogashira conditions to obtain polymer **17** (M_n = 20 000).

Simple inspection of the absorption and emission spectra for both the meta family (**14** and **15**) and the para family (**16** and **17**) reveals the electronic effects of chromophore planarization (Figures 5 and 6). When compared to the conformationally flexible **15** and **16**, the more rigid, aromatized units present in **14** and **17** offer more defined vibronic structure and significant reduction in energy between the (0,0) absorption and the emission λ_{max}. The relative oscillator strengths for the low-energy absorbances of meta polymer **14** have lower intensities when compared to the analogous low-energy absorptions for para **17**. While significantly altering the absorption profiles, monomer aromatization within a family only results in a slightly red-shifted emission maximum (meta: 14 nm; para: 10 nm). Despite the differences in ground-state geometries within both families of polymers, these close resemblances in emission λ_{max} indicate similar excited-state energetics among the flexible and

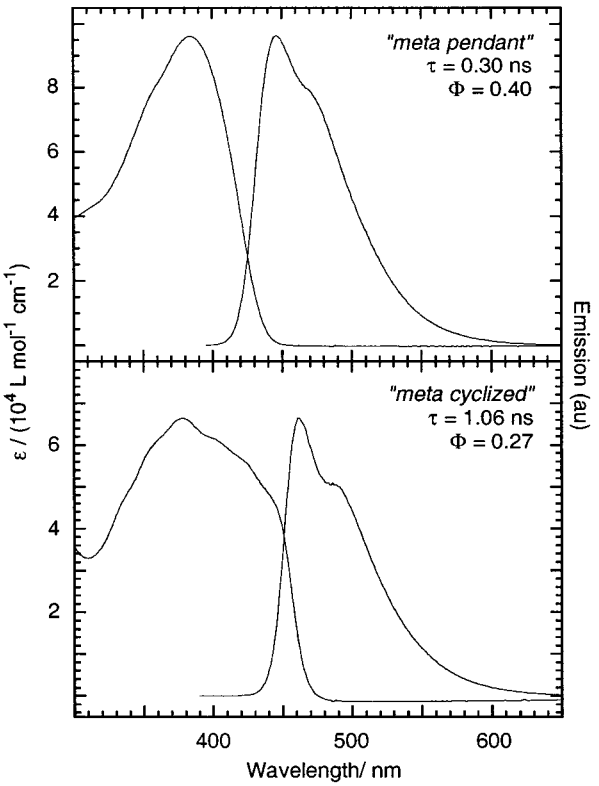

Figure 5. Absorption and emission spectra for **15** (top) and **14** (bottom) acquired at room temperature in CH_2Cl_2. Quantum yields were measured relative to quinine sulfate in 0.1 N H_2SO_4 (f = 0.55); lifetimes were determined by phase modulation. ϵ was reported per monomer repeat unit.

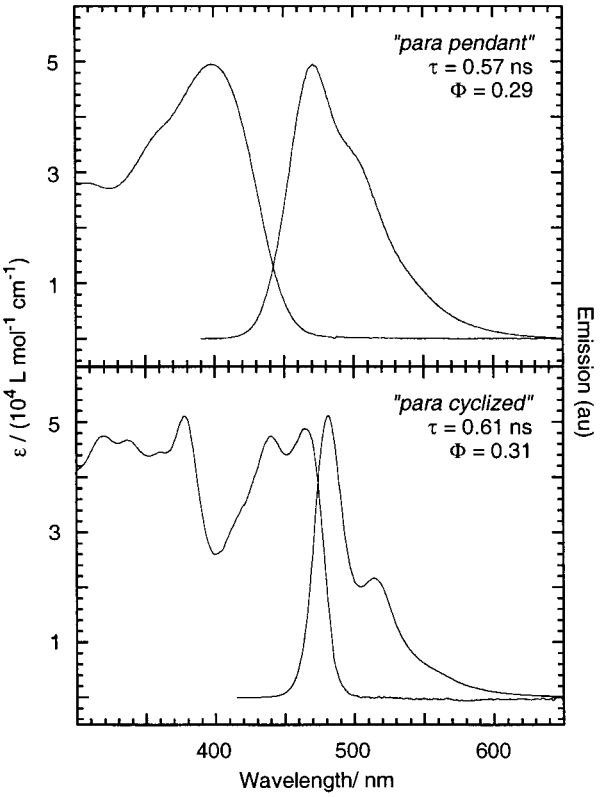

Figure 6. Absorption and emission spectra for **16** (top) and **17** (bottom) acquired at room temperature in CH_2Cl_2. Measurements as in Figure 5.

(21) For $FeCl_3$ polymerizations of the base 1,4-di(2-thienyl)benzene moiety, see: Reynolds, J. R.; Ruiz, J. P.; Child, A. D.; Nayak, K.; Marynick, D. S. *Macromolecules* **1991**, *24*, 678−687.

Scheme 8[a]

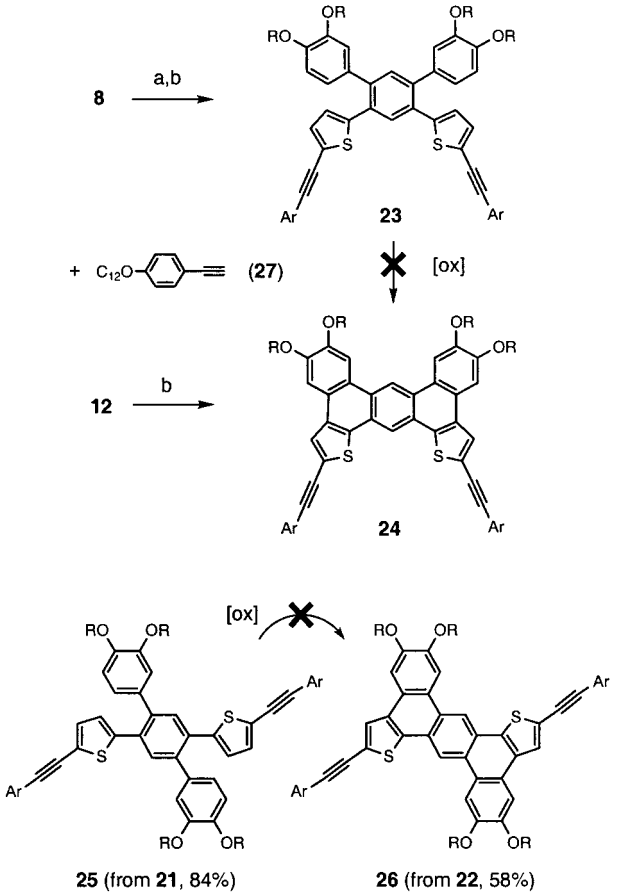

[a] R = 2-ethylhexyl, Ar = 4-(*n*-$C_{12}H_{25}O$)C_6H_4-. Reagents and conditions: (a) i. $Hg(OAc)_2$, ii. I_2, CH_2Cl_2, room temperature; (b) **27**, $(Ph_3P)_2PdCl_2$, CuI, THF/ DIPA, 50 °C.

the rigidified polymers. This supports the fact that the pendant arenes of noncyclized **15** and **16** become more planarized after initial excitation in order to allow for greater excited state delocalization. The slightly blue-shifted emissions observed in the pendant systems (**15** and **16**) indicate a minor persistence of localized poly(phenylene) character in their excited states. This would suggest that charge localization still exists on phenylene (or thienylene) segments despite any excited-state planarization effects.

With both isomeric sets of polymers displaying absorption and emission characteristics expected after incorporating a more rigid aromatic chromophore, we measured the fluorescence lifetimes and quantum yields of these polymers. Pendant meta polymer **15** had a solution lifetime of 0.30 ns ($\Phi = 0.40$) whereas aromatized **14** displayed a lifetime of 1.06 ns ($\Phi = 0.27$), a 3.5-fold larger value. A correlation of the lifetimes with the quantum yield measurements indicated a decreased rate of radiative decay for the aromatized **14** relative to **15**. In contrast, para polymers **16** and **17** exhibited *identical* solution lifetimes (0.57 and 0.61 ns, respectively) and quantum yields ($\Phi = 0.29$ and 0.31, respectively), suggesting that the inclusion of the aromatized system effects no significant change in the radiative rate. We have assumed that the meta systems exist in disordered chain conformations; however, the geometric constraints imposed by the meta orientation may possibly allow for intrachain interactions. We therefore needed to examine systems where chain dynamics would not offer complications.[22]

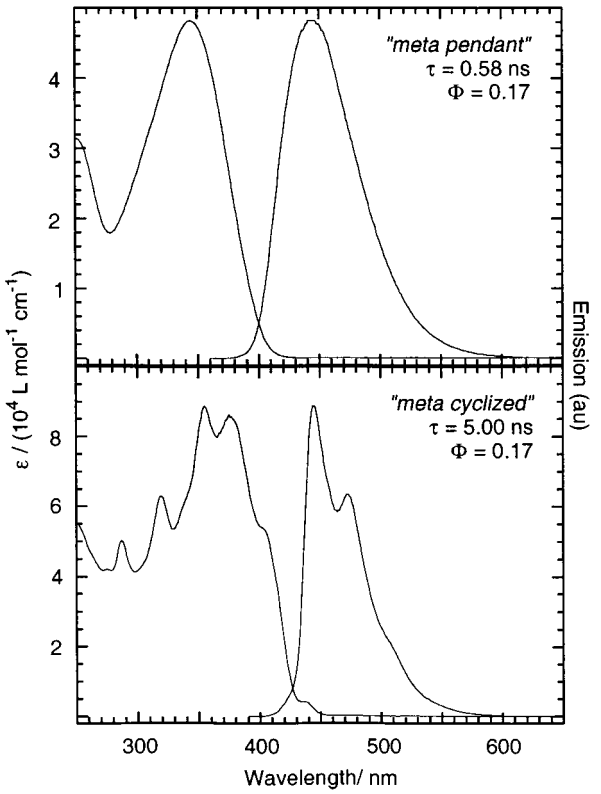

Figure 7. Absorption and emission spectra for **23** (top) and **24** (bottom) acquired at room temperature in CH_2Cl_2. Measurements as in Figure 5.

To further investigate the interplay between chromophore aromaticity and symmetry, we synthesized alkynylated meta models **23** and **24** and the related para derivatives **25** and **26** as shown in Scheme 8. Unlike the polymers, these systems possess shorter, well-defined conjugation lengths thus allowing for a clear assessment of planarization effects within molecular systems without significant contributions from conformational variations in effective conjugation lengths. While we initially anticipated the use of oxidative cyclizations to obtain the alkynyl-appended polycyclic aromatics (e.g. **23** to **24**), extensive decomposition during the reaction led to unidentifiable materials, apparently a result of alkyne degradation.[23] However, despite the problematic purification of the para bromide **22**, Sonogashira cross-coupling of the respective dihalides with alkyne **27**[24] provided all four alkynylated models in high yields.

In agreement with the optical trends observed for the polymer systems, the aromatized systems **24** and **26** displayed sharper vibronic structure and decreased Stokes' shifts when compared to the pendant analogues **23** and **25** (Figures 7 and 8). Again in

(22) At this time, we cannot rule out macromolecular conformations within the meta polymer systems that may allow for intrapolymer cross-talk by way of helical "kinked" segments in solution analogous to the work of Moore. However, we would expect that such helical conformations would contribute minimally to the macromolecular architecture given our choice of spectroscopic solvent. The model systems (compounds **23**−**26**) also affirm the photophysical effects of chromophore rigidity in the absence of macromolecular conformational issues or effective conjugation length disparities. For a seminal study of solvent-driven "zigzag" to helix conformational changes with related *m*-phenylene ethylene oligomers, see: Nelson, J. C.; Saven, J. G.; Moore, J. S.; Wolynes, P. G. *Science* **1997**, *277*, 1793−1796.

(23) Cyclic voltammetric studies of **23** and **25** show a lack of new electroactive products formed near the electrode surface as well as complete anodic irreversibility over a range of potential scan rates (0.1−10 V/s). Please see the Supporting Information for CVs taken at 100 mV/s for **23** and **25** (Supplemental Figure 1).

(24) Goldfinger, M. B.; Swager, T. M. *J. Am. Chem. Soc.* **1994**, *116*, 7895−7896.

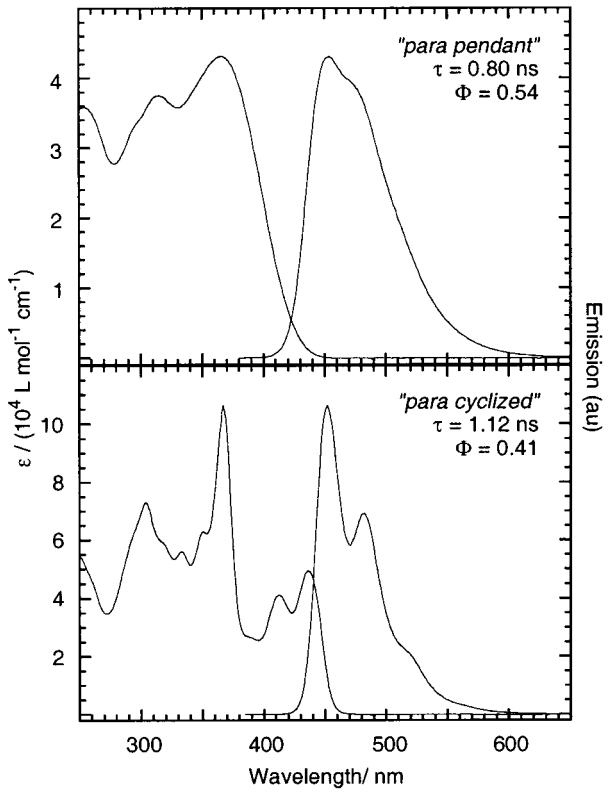

Figure 8. Absorption and emission spectra for **25** (top) and **26** (bottom) acquired at room temperature in CH_2Cl_2. Measurements as in Figure 5.

line with the polymer electronic properties, the low oscillator strength of the (0,0) absorption observed for **24** (436 nm, log $\epsilon = 3.63$) when compared to that in **26** (also at 436 nm, log $\epsilon = 4.69$) indicates a much more weakly allowed process. We then measured the fluorescence lifetimes and quantum yields for these molecular systems of shorter and more defined conjugation lengths. Consistent with the polymeric systems, we found a near 9-fold increase in lifetime in the cyclized meta system (**23**: 0.58 ns; **24**: 5.00 ns) while the quantum yield remained equal ($\Phi = 0.17$). The cyclized para system displayed a much less pronounced extension upon planarization (**25**: 0.80 ns; **26**: 1.12 ns) while the quantum yield decreased (**25**: 0.54; **26**: 0.41). For both systems, the decreases in radiative rates upon planarization within an isomeric family give rise to the lifetime extensions.

These results stand in agreement with similar lifetime enhancements resulting from symmetry-forbidden transitions in conjugated polymers containing triphenylene cores.[18b] In line with our earlier findings related to the electrochromicity and conductivity of poly(**2**),[9] the set of para model systems (**25** and **26**) and the related para polymers (**16** and **17**) appear to maintain much longer excited-state conjugation pathways localized through the thienyl−aryl−thienyl segments despite any structural rigidification. As such, the differences in radiative rates in the planarized para **17** are not as severe as are those in the less delocalized meta systems. Ridigification provides a consistent explanation for the observed changes in optical properties upon chromophore aromatization, but the lack of significant excited-state lifetime enhancement within the planarized para **17** indicates that simple rigidification of a given chromophore does not necessarily couple to an increase in lifetime. Our ongoing studies will assess the physical properties of these molecular ensembles as well as continue to investigate the effects of repeat unit aromatization on enhancing excited-state lifetimes in systems of other symmetries. Future work will measure the extent of exciton migration through these and other related polymers in an effort to study and exploit such systems as new sensory materials.

Conclusions

We have shown that oxidative couplings of pendant thienyl moieties allow for construction of discrete molecular structures as a complement to well-established arene-based molecular cyclizations and to thiophene-based polymerization strategies. The ease of synthesis for these large polycyclic aromatics and their pendant aromatic precursors has allowed us to further study and expand upon a cyclization/polymerization strategy we recently described by providing a powerful route to electroactive and emissive aromatic structures. We have demonstrated both the α- and the β-sites of pendant monomers may undergo cyclization under oxidative conditions and have applied this to the synthesis of a variety of large thiophene-based polycyclics from readily synthesized pendant aromatics. By incorporating the thiophene moieties, we included a synthetic handle to access even more elaborate scaffolds. We then used this chemistry as a platform to demonstrate the effects of chromophore aromatization on photophysical properties of conjugated polymers. From these studies, we have established further structural groundwork to aid in the design of new sensory materials. We will report ongoing studies related to the liquid crystallinity and OFET behavior of these new materials in due course.

Acknowledgment. We appreciate financial support provided by the Army Research Office through a MURI award (Tunable Optical Polymer Systems). We thank Dr. Jeff Simpson (MIT DCIF) for assistance and advice with ROESY experiments.

Supporting Information Available: Experimental procedures and characterization data for all new compounds and CVs of **23** and **25** (PDF). This material is available free of charge via the Internet at http://pubs.acs.org.

JA0262636